Dynamic mode theory of optical resonators undergoing refractive index changes

Brian A. Daniel,[1,*] Drew N. Maywar,[2] and Govind P. Agrawal[1]

[1]*The Institute of Optics, University of Rochester, Rochester, New York 14627, USA*
[2]*Electrical, Computer and Telecommunications Engineering Technology Department, Rochester Institute of Technology, Rochester, New York 14623, USA*
**Corresponding author: daniel@optics.rochester.edu*

Received July 5, 2011; accepted July 27, 2011;
posted August 2, 2011 (Doc. ID 150395); published August 23, 2011

We present a theoretical model describing the dynamics of the electromagnetic field in an optical resonator undergoing refractive index changes. We use an operator formulation of Maxwell's equations with a standard time-dependent perturbation theory to derive the dynamic mode-amplitude equations that govern the response of a resonator to a perturbing dipole-moment density. We show that in the case of time-dependent changes in the refractive index, a coupling matrix $\Gamma_{km}(t)$ that appears in the equations accounts for all novel physical processes that can be expected to occur. In particular, the phenomenon of adiabatic wavelength conversion is governed by the diagonal elements of this matrix, and the off-diagonal elements are responsible for the transfer of energy from an excited resonator mode into its neighboring modes. Our model clearly shows that the latter process can occur only when the index changes are spatially nonuniform. We discuss the spatially uniform and nonuniform cases separately and compare the predictions of our model with experimental data available in the literature. The overall good agreement suggests that this model should be useful in the study of dynamic optical resonators. Moreover, since we do not make any assumptions about the type of dielectric cavity used, the width of input pulses, or the speed with which the refractive index is changed, this model should be applicable under most experimental situations.

OCIS codes: 130.0130, 130.7405, 230.0230, 070.5753.

1. INTRODUCTION

Adiabatic wavelength conversion (AWC) is a recently discovered phenomenon that can occur in optical resonators and has the potential to be used for electrically or optically controllable wavelength conversion. AWC occurs when the refractive index of a resonator is changed while it is filled with light. The frequency of the optical field within the cavity follows the resulting change in resonance frequency in a manner that has been compared to the tuning of a guitar string after it has been plucked [1]. The resulting extent of wavelength conversion depends only on the amount of the refractive index change and is independent of the means, which can be an electro-optic effect (injection of free charge carriers in a semiconductor, the Pockels effect, etc.) or a purely optical effect (free carrier generation through optical absorption, cross-phase modulation, etc.). That AWC can be implemented with an electro-optic effect is a distinct advantage over other wavelength-conversion schemes which typically rely on optical nonlinearities and therefore require high-power-consumption devices. Not only is AWC promising for energy efficient wavelength-conversion devices, such devices may also be electrically reconfigurable because the extent of wavelength conversion depends only on the magnitude of the change in the refractive index.

AWC was first discussed in 2005 by Yanik and Fan [2] and later studied in more detail by Notomi and Mitsugi using a finite-difference time-domain (FDTD) numerical technique [1]. Preble *et al.* first demonstrated AWC experimentally in 2007 [3]. Since then, the AWC phenomenon has attracted considerable attention [4–14]. Three different theoretical approaches to AWC in optical resonators have been taken in the literature. The earliest studies relied primarily on FDTD simulations [1,4,5] which are time consuming to perform and limited in the insight they can offer. A modal-expansion approach was also outlined in [15] and applied to understanding the conditions under which different resonator modes will be coupled in the presence of refractive index changes, and which also describes AWC. This approach was originally proposed for understanding the effects of refractive index changes in photonic-crystal waveguides and has also been used for that purpose [6,16,17]. More recently, an intuitive linear systems approach has been developed which offers considerable physical insight and has been used to study the temporal and spectral changes of optical pulses undergoing AWC [7].

In this paper we present a modal-expansion approach to dynamic refractive index changes in resonators that is similar to the one outlined in [15] but offers two important advantages. First, we find that by choosing a different set of fields with which to expand the cavity modes we are able to cast the perturbation into a general dipole-moment density $\mathbf{P}^{(p)}$, which allows for the incorporation of a variety of other effects such as those associated with optical nonlinearities and gain. Second, we include in our theory coupling to an input field and resonator losses, which allows for comprehensive modeling of the system dynamics. In Section 2 we use Maxwell's equations to derive the dynamic mode-amplitude equations which govern the response of an optical resonator to a perturbation. In Section 3 we use this theory to study AWC and compare the predictions of our theory with experimental results from the literature. In Section 4 we use our theory to study the phenomenon of dynamic mode coupling

which can occur in conjunction with AWC under certain conditions, and we compare its predictions with an experimental result from the literature.

2. THEORETICAL FRAMEWORK

In this section we first present an operator formulation of Maxwell's equations that enables us to write them as a single equation which is similar to the Schrödinger equation. The resonant modes of a cavity correspond to the eigenstates of a Hermitian operator. Dynamic changes in the refractive index are treated as perturbations to these resonant modes. The use of the standard time-dependent perturbation theory then leads to a set of ordinary differential equations for their amplitudes. The framework developed here is quite general and can be applied to a wide range of problems in resonator optics, including nonlinear optical interactions and material-resonance phenomena (lasers and amplifiers).

A. Operator Form of Maxwell's Equations

We consider an optical resonator containing a material whose dielectric constant can change with time from its static value $\epsilon(\mathbf{r})$ such that

$$\epsilon'(\mathbf{r},t)=\epsilon(\mathbf{r})+\Delta\epsilon(\mathbf{r},t), \tag{1}$$

where $\Delta\epsilon$ represents a time-dependent change in the dielectric permitivitty induced by external means (e.g., by injection of free carriers or an electro-optic effect). Maxwell's equations in the time domain can be written in the form

$$\nabla\times\mathbf{E}=-\mu_0\frac{\partial\mathbf{H}}{\partial t},\qquad \nabla\times\mathbf{H}=\epsilon_0\epsilon(\mathbf{r})\frac{\partial\mathbf{E}}{\partial t}+\frac{\partial\mathbf{P}^{(p)}}{\partial t}. \tag{2}$$

The dynamic refractive index changes are included through a time-dependent perturbation to the material polarization in the form $\mathbf{P}^{(p)}=\epsilon_0\Delta\epsilon(\mathbf{r},t)\mathbf{E}$. In the following analysis, we employ the complex representation of an electromagnetic field in the form of an analytic signal.

It was shown in [18] for unperturbed dielectric cavities that Maxwell's equations can be formulated as the following operator equation that describes the temporal evolution of an electromagnetic field in an abstract vector space in a manner analogous to the Schrödinger equation in quantum mechanics:

$$i\frac{\partial}{\partial t}|\psi\rangle=\hat{M}|\psi\rangle+|V(t)\rangle. \tag{3}$$

The field states are related to the electric and magnetic fields as

$$|\psi\rangle=\begin{pmatrix}\sqrt{\epsilon_0}\mathbf{E}\\ \sqrt{\mu_0}\mathbf{H}\end{pmatrix},$$

where the permitivitty and permeability of free space are incorporated so as to give the vector components the same units. The inner product between two elements of the vector space is defined as

$$\langle\psi_a|\psi_b\rangle=\frac{1}{4}\int[\epsilon_0\epsilon(\mathbf{r})\mathbf{E}_a^*\cdot\mathbf{E}_b+\mu_0\mathbf{H}_a^*\cdot\mathbf{H}_b]\mathrm{d}^3\mathbf{r}. \tag{4}$$

The operator $\hat{M}$ driving the time evolution of the electromagnetic field has the form

$$\hat{M}=\begin{pmatrix}0 & i\frac{c}{\epsilon}\nabla\times\\ -ic\nabla\times & 0\end{pmatrix}.$$

It is easily shown that $\hat{M}$ is Hermitian under the inner product given in Eq. (4). Finally, perturbations resulting from dynamic refractive index changes are incorporated in Eq. (3) through $|V(t)\rangle$, which is given as

$$|V(t)\rangle=\begin{pmatrix}\frac{-i}{\epsilon\sqrt{\epsilon_0}}\frac{\partial\mathbf{P}^{(p)}}{\partial t}\\ 0\end{pmatrix}. \tag{5}$$

We assume that the solutions of Eq. (3) in the absence of perturbation (i.e., when $|V(t)\rangle=0$) are known. This is equivalent to finding the resonator modes for a given cavity configuration in the form $|\psi_k(t)\rangle=e^{-i\omega_k t}|\omega_k\rangle$, where $|\omega_k\rangle$ is an eigenstate of the operator $\hat{M}$, i.e.,

$$\hat{M}|\omega_k\rangle=\omega_k|\omega_k\rangle.$$

Here ω_k is the resonance frequency of the kth resonator mode. If $\mathbf{e}_k(\mathbf{r})$ and $\mathbf{h}_k(\mathbf{r})$ are the electric and magnetic fields associated with this mode, the eigenvector $|\omega_k\rangle$ in our notation is given by

$$|\omega_k\rangle=\begin{pmatrix}\sqrt{\epsilon_0}\mathbf{e}_k\\ \sqrt{\mu_0}\mathbf{h}_k\end{pmatrix}. \tag{6}$$

Since the operator $\hat{M}$ is Hermitian, resonator modes oscillating at different frequencies are orthogonal:

$$\langle\omega_k|\omega_m\rangle=N_m\delta_{km},$$

where N_m is a normalization factor. For monochromatic solutions of Maxwell's equations, the electric energy is equal to the magnetic energy, allowing us to express N_m in terms of the electric field only:

$$N_m=\frac{1}{2}\int\varepsilon_0\epsilon(\mathbf{r})|\mathbf{e}_m|^2\mathrm{d}^3\mathbf{r}.$$

We emphasize that our formalism describes any conceivable dielectric cavity, including microring resonators, photonic-crystal cavities, whispering-gallery mode resonators, etc.

B. Time-Dependent Perturbation Theory

To solve Eq. (3), we apply the standard time-dependent perturbation theory of quantum mechanics and assume that the solution $|\psi(t)\rangle$ for the perturbed electromagnetic field can be expanded in terms of the unperturbed modes (eigenstates) of the resonator. In general, one should include radiation modes because some fraction of the optical field is radiated out of the cavity in any real resonator. In the case of relatively high-Q cavities, however, the dominant contribution to the electromagnetic field is from the resonantly enhanced discrete cavity modes, and we are justified in including only these modes in the expansion

$$|\psi(t)\rangle=\sum_m\frac{a_m(t)}{\sqrt{N_m}}|\omega_m\rangle, \tag{7}$$

where $a_m(t)$ is the amplitude of the mth mode at time t. The normalization factor N_m ensures that $\sum_m |a_m(t)|^2$ is the total electromagnetic energy stored in the cavity at any given moment in time, and $|a_k(t)|^2$ is the energy stored in the kth cavity mode.

By inserting the solution form Eq. (7) into Maxwell's equation [3] and multiplying from the left by $\langle \omega_k |$, we arrive at the following differential equation describing the temporal evolution of the mode amplitude a_k:

$$\frac{da_k}{dt} = -i\omega_k a_k - \frac{1}{4\sqrt{N_k}} \int \mathbf{e}_k^* \cdot \frac{\partial \mathbf{P}^{(p)}}{\partial t} \mathrm{d}^3\mathbf{r}. \tag{8}$$

There are two properties of optical resonators that must be taken into account in a complete model of the system dynamics: the finite photon lifetime of cavity modes and coupling to an external input field. Although both of these can in principle be incorporated in Eq. (8) through a suitable external perturbing polarization $\mathbf{P}^{(p)}$, such an approach is too complicated to be useful. In Appendix A, we present a phenomenological approach for introducing these two effects in Eq. (8) and show that it takes the form

$$\frac{da_k}{dt} = -i\omega_k a_k - \frac{1}{2\tau_{ph}^k} a_k + \kappa_k A_{in}(t) - \frac{1}{4\sqrt{N_k}} \int \mathbf{e}_k^* \cdot \frac{\partial \mathbf{P}^{(p)}}{\partial t} \mathrm{d}^3\mathbf{r}, \tag{9}$$

where τ_{ph}^k is the photon lifetime of the kth mode and $A_{in}(t)$ is the input field, normalized such that $|A_{in}|^2$ is the optical power. The coupling coefficient is defined as $\kappa_k = \sqrt{T_k/\tau_r}$, where τ_r is the round-trip time within the resonator and T_k is the fraction of input light coupling into the resonator mode at frequency ω_k. For example, if a mirror is used to couple input light into the resonator, T_k is just the transmittance of that mirror.

Equation (9) is the dynamic mode-amplitude equation. It is quite general and can be used to describe a wide range of linear and nonlinear effects in optical resonators. It has been derived before in the context of nonlinear optical interactions in microring and microdisk resonators by making use of the Helmholtz equation [19,20]. The technique we use to derive it in this paper demonstrates that it is applicable to all kinds of dielectric resonator cavities, and forgoes the use of the slowly varying envelope approximation. Here we use it to describe the influence of dynamic changes in the refractive index of a material used to form the resonator. In this case, the perturbing polarization has the form

$$\begin{aligned} \mathbf{P}^{(p)}(\mathbf{r},t) &= \epsilon_0 \Delta\epsilon(\mathbf{r},t)\mathbf{E}(\mathbf{r},t) \\ &= \epsilon_0 \Delta\epsilon(\mathbf{r},t) \sum_m \frac{a_m(t)}{\sqrt{N_m}} \mathbf{e}_m(\mathbf{r}). \end{aligned} \tag{10}$$

Using Eq. (10) in Eq. (9). we obtain a set of coupled amplitude equations in the form

$$\begin{aligned} \frac{da_k}{dt} = &-i\omega_k a_k - \frac{1}{2\tau_{ph}^k} a_k + \kappa_k A_{in}(t) \\ &- \sum_m \left(\frac{d\Gamma_{km}}{dt} a_m + \Gamma_{km} \frac{da_m}{dt} \right), \end{aligned} \tag{11}$$

where Γ_{km} are the elements of the dynamic coupling matrix and are given by

$$\Gamma_{km}(t) = \frac{\int \Delta\epsilon(\mathbf{r},t)\mathbf{e}_k^*(\mathbf{r}) \cdot \mathbf{e}_m(\mathbf{r}) \mathrm{d}^3\mathbf{r}}{\left(4 \int \epsilon(\mathbf{r}) |\mathbf{e}_k(\mathbf{r})|^2 \mathrm{d}^3\mathbf{r} \int \epsilon(\mathbf{r}) |\mathbf{e}_m(\mathbf{r})|^2 \mathrm{d}^3\mathbf{r}\right)^{1/2}}. \tag{12}$$

Equation (11) describes how the amplitude a_k of a specific resonator mode evolves in response to dynamic index changes while driven with an incident field $A_{in}(t)$. Time-dependent changes in the refractive index not only affect a_k, but they can also couple this mode to other resonator modes, resulting in their excitation, even when the input field is tuned to excite only a single resonance.

C. Comparison with Other Theories in the Literature

A similar modal-expansion approach to Maxwell's equations has been used elsewhere in the literature to understand the effects of dielectric perturbations in photonic crystals [6,16,17] as well as optical resonators [15]. This approach was originally formulated in [16] to study the coupling of propagating modes in a photonic-crystal waveguide. It was later pointed out that the same formulation can be applied to understand mode-coupling phenomena in optical resonators [15]. Our theory differs from this approach in two important ways. First, we have chosen to expand the electromagnetic modes in terms of the **E** and **H** fields as opposed to the **D** and **H** fields. This is a subtle difference but the resulting theory turns out to be applicable to a much wider range of phenomena. This is because we are able to cast the perturbation in terms of a dipole-moment density $\mathbf{P}^{(p)}$, which can readily incorporate phenomena associated with optical nonlinearities, material resonances, etc., whereas the previous approach was limited to perturbations of the material permitivitty, $\Delta\epsilon$. Second, we have incorporated into our theory important effects associated with optical resonators such as the finite photon lifetime and coupling to an external input field. This allows us to perform comprehensive numerical modeling of the cavity dynamics, whereas the previous modal-expansion approach had been applied to optical resonators solely for understanding the nature of the terms associated with the intermode coupling [15].

If some typically valid approximations are made, our theory leads to the same coupling coefficients that were derived in [16]. In particular, if we make the approximation $da_m/dt \approx -i\omega_m a_m$ on the right side of Eq. (11), and further assume that the index changes occur on a time scale much longer than the optical period so that $|d\Gamma_{km}/dt| \ll |\omega_m \Gamma_{km}|$, then this equation reduces to

$$\frac{da_k}{dt} = -i\omega_k a_k - \frac{1}{2\tau_{ph}^k} a_k + \kappa_k A_{in}(t) + \sum_m i\Gamma_{km}\omega_m a_m. \tag{13}$$

It can be shown that the mode-coupling terms within the sum in Eq. (13) are equivalent to the ones derived in [16] using the alternative modal-expansion approach.

3. ADIABATIC WAVELENGTH-CONVERSION

AWC always occurs in the presence of dynamic refractive index changes. In our formulation, this process is described by Eq. (11) through the diagonal matrix element Γ_{kk}, i.e, the term

for which $m = k$ in the sum is responsible for AWC. To see this more clearly, consider the special case where only a single resonator mode (say, the qth mode) is excited by the input field and coupling to other modes either does not occur or can be neglected. The set Eq. (11) then reduces to the following single equation describing the mode dynamics:

$$[1+\Gamma(t)]\frac{da_q}{dt} = -i\omega_q a_q - \left(\frac{1}{2\tau_{ph}^q} + \frac{d\Gamma}{dt}\right)a_q + \kappa_q A_{in}(t), \quad (14)$$

where $\Gamma = \Gamma_{qq}$ is defined as

$$\Gamma(t) = \frac{\int \Delta\epsilon(\mathbf{r},t)|\mathbf{e}_q|^2 d^3\mathbf{r}}{2\int \epsilon(\mathbf{r})|\mathbf{e}_q|^2 d^3\mathbf{r}}. \quad (15)$$

A. Interpretation of the Dynamical Equation

Consider what happens after an input field has excited the resonant mode and then turns off. Neglecting the last term in Eq. (14), we can write it in the form

$$\frac{da_q}{dt} = -i\omega_q'(t)a_q - \gamma(t)a_q, \quad (16)$$

where

$$\omega_q'(t) = \frac{\omega_q}{1+\Gamma(t)}, \qquad \gamma(t) = \left(\frac{1}{2\tau_{ph}^q} + \frac{d\Gamma}{dt}\right)\frac{1}{1+\Gamma(t)}. \quad (17)$$

The physical meaning of this equation is quite clear. It shows that the electromagnetic field inside the cavity oscillates at a new frequency $\omega_q'(t)$ that changes with time and decays at a rate $\gamma(t)$. The new oscillation frequency of the mode can be approximated by noting that Γ is typically much smaller than 1 as

$$\omega_q'(t) \approx \omega_q[1-\Gamma(t)]. \quad (18)$$

In the case where the resonator medium has a uniform refractive index n_0 that is changed dynamically by an amount $\Delta n(t)$ over the entire mode volume, we can make the approximation $\Gamma(t) \approx \Delta n(t)/n_0$. In this case the change in the optical frequency produced through AWC is given by $\Delta\omega \approx -\omega_q(\Delta n/n_0)$. This expression for the frequency shift has been known since the first theoretical studies of AWC [1,2] and has also been verified experimentally [4].

In addition to the frequency shift, Eq. (17) indicates that the decay rate of the cavity mode changes while the refractive index is changing through the term $d\Gamma/dt$. This implies that the optical energy stored in the resonator also changes with time. Using the solution for the electromagnetic field in Eq. (7) (when only one mode is considered), the stored energy is found to be

$$U(t) = \frac{1}{4}\int [\epsilon_0\epsilon'(\mathbf{r},t)|\mathbf{E}|^2 + \mu_0|\mathbf{H}|^2]d^3\mathbf{r} = [1+\Gamma(t)]|a_q|^2. \quad (19)$$

Taking the time derivative of $U(t)$ and using Eq. (16), we obtain the following differential equation:

$$\frac{dU}{dt} = -\frac{U d\Gamma/dt}{1+\Gamma(t)} - \frac{U}{\tau_{ph}^q(1+\Gamma)}.$$

Assuming that the input field turns off at $t = 0$ this equation has the solution

$$U(t) = \frac{U_0}{1+\Gamma(t)}\exp\left[-\frac{1}{\tau_{ph}^q}\int_0^t \frac{dt'}{1+\Gamma(t')}\right]. \quad (20)$$

The electromagnetic energy stored in the cavity is clearly not a conserved quantity during the AWC process. One of the reasons for this is the finite photon lifetime of the resonator represented by the exponential term in Eq. (20). Equation (20) indicates that there is also another source of energy change in a dynamic resonator. To see this more clearly, consider a time scale that is much shorter than the photon lifetime so that the exponential term can be replaced with 1. The mode energy U is still not conserved because of the factor in the denominator. These intrinsic energy changes were first noted in [1]. In that work it was found through FDTD calculations that when the photon lifetime is long enough the optical energy is not conserved, but that the number of photons in the cavity is. Using $U(t) = U_0/(1+\Gamma)$ and Eq. (17), one can see that the number of photons N_p stored in the cavity,

$$N_p = U(t)/\hbar\omega_q'(t) = U_0/\hbar\omega_q, \quad (21)$$

is indeed conserved, in agreement with the numerical simulations.

B. Comparison with Experimental Results

In order to test the validity of our theory, we compare its predictions with experimental results reported by Preble *et al.* in [3]. In their experiment, a silicon ring resonator was employed in the add/drop configuration depicted in Fig. 1. After an 18 ps probe pulse at the 1564 nm wavelength was launched into the resonator through the input waveguide, the refractive index was decreased in a dynamic fashion, and a blue-shifted signal was observed at the drop port. The index change was induced by generating electron-hole pairs through optical absorption of a 100 fs pump pulse at the 415 nm wavelength. The pump pulse was focused onto the resonator from above through a free-space objective. The 10 μm spot size of the focused pump pulse was larger than the ring's 6 μm diameter. This resulted in a uniform distribution of charge carriers in the ring and therefore a uniform change in the refractive index.

We model the refractive index change using the semiempirical model developed by Soref and Bennett [21]. In that work it was predicted that the refractive index change in the 1.55 μm wavelength regime induced by free-charge carriers in silicon can be expressed as

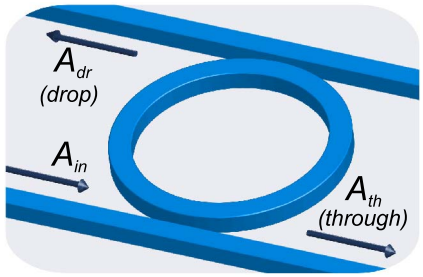

Fig. 1. (Color online) Schematic of a silicon add/drop resonator

$$\Delta n = -\sigma_n^e N - (\sigma_n^h N)^{4/5} + i\frac{\sigma_a}{2k_0}N, \tag{22}$$

where N is the number density of electron-hole pairs. $\sigma_n^e = 8.8\times10^{-22}\,\mathrm{cm}^2$, $\sigma_n^h = 4.6\times10^{-22}\,\mathrm{cm}^3$, $\sigma_a = 14.5\times10^{-18}\,\mathrm{cm}^2$, and $k_0 = 2\pi/\lambda$. Note that the change in the refractive index is complex because the generated carriers absorb light near $1.55\,\mu$m. Because the index change in the cavity is uniform we make the approximation $\Gamma(t) \approx \Delta n(t)/n_0$, where $n_0 = 3.5$ is the refractive index of silicon at the probe wavelength.

The carrier density can be obtained by solving the rate equation

$$\frac{dN}{dt} = \frac{\xi P_p(t)}{V_{\mathrm{cav}}\hbar\omega_p} - \frac{N}{\tau_{fc}}, \tag{23}$$

where $P_p(t)$ is the optical power of the pump pulse assumed to have a Gaussian shape, ξ is the fraction of the pump power absorbed by the resonator, V_{cav} is the volume of the cavity, $\hbar\omega_p$ is the energy of a photon at the pump wavelength, and τ_{fc} is the free-carrier lifetime. In our simulations, τ_{fc} is taken to be infinite since the dynamics that we are interested in occur on a much shorter time scale.

The transmitted signal at the drop port of the resonator (A_{dr} in Fig. 1) is related to the mode amplitude by

$$A_{dr}(t) = \kappa_q a_q(t), \tag{24}$$

where κ_q is the same as in Eq. (9) for a symmetric resonator [22]. Note that $|A_{dr}(t)|^2$ is the optical power in the output waveguide.

Figures 2 and 3 compare the experimentally measured drop-port spectra reported in [3] with the output spectra predicted by our model under a variety of experimental conditions. We stress that not a single fitting parameter was used in the calculations for the output optical spectra in Fig 2 as well as the spectra in Figs. 3(a) and 3(b); all of the relevant parameters were reported in [3] and are recorded in Table 1. In Fig. 3(c) we had to use one fitting parameter because the temporal delay between the pump and probe pulses was not given in [3] for this particular experimental scenario. All optical spectra in Figs. 2 and 3 have been normalized to the spectral peak of the probe pulse at the drop port of the resonator in the absence of a pump pulse.

Figure 2 shows the experimental [3] and calculated spectra for two different pump-pulse energies (E_p). The total absorbed energy of each pump pulse (ξE_p) is 0.419 pJ in Fig.2(a) and 1.38 pJ in Fig.2(b). As expected, the probe experiences more spectral blue shift for a larger pump-pulse energy (the index is changed by a greater amount), and the AWC efficiency is likewise decreased because of increased absorption from the larger number of free carriers. While the qualitative features are in

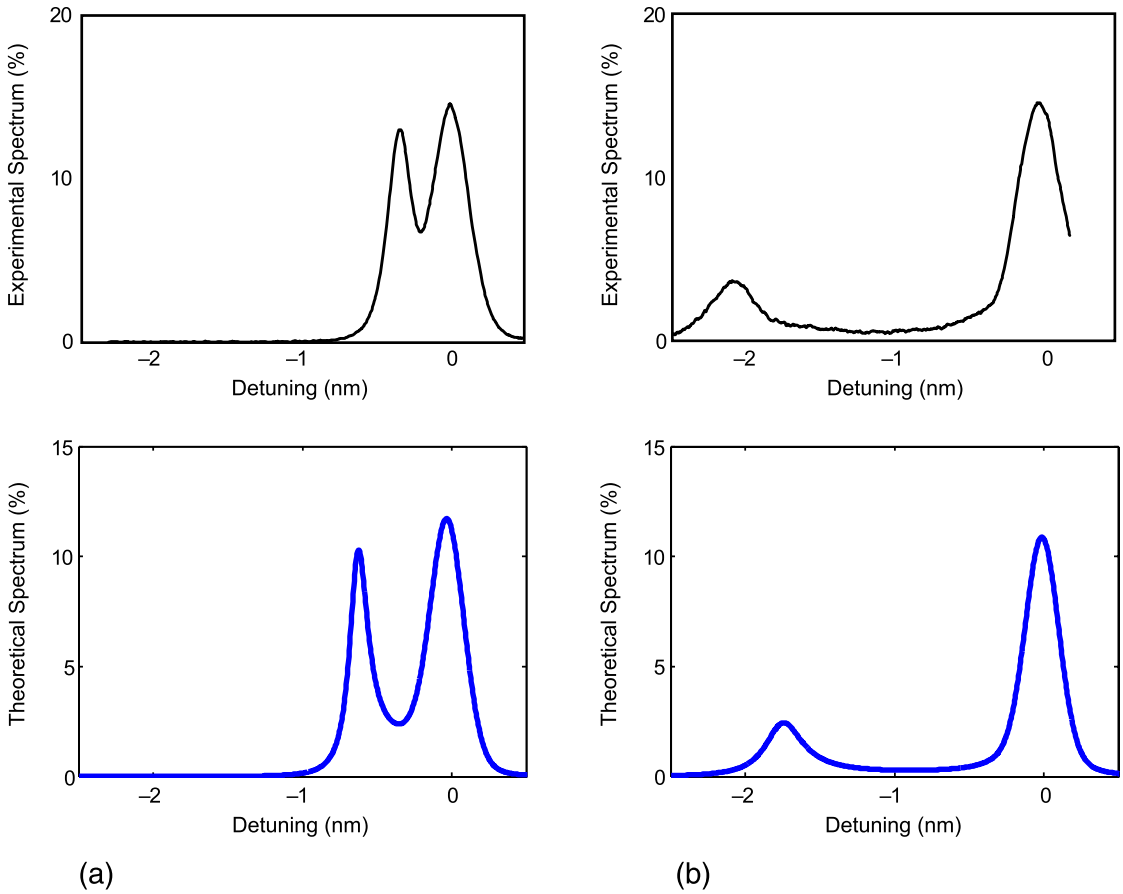

Fig. 2. (Color online) Comparison with experimental results from the literature for AWC in a silicon ring resonator. Measured drop-port spectra from [3] are compared with theoretical drop-port spectra predicted by Eq. (14) under the same experimental conditions. No fitting parameters were used in the simulations; all of the necessary information was reported in [3]. The absorbed pump energies in (a) and (b) are 0.419 and 1.38 pJ respectively. All other parameters are recorded in Table 1. The experimental spectra are adapted from [3] with permission from Macmillan Publishers Ltd., copyright 2007.

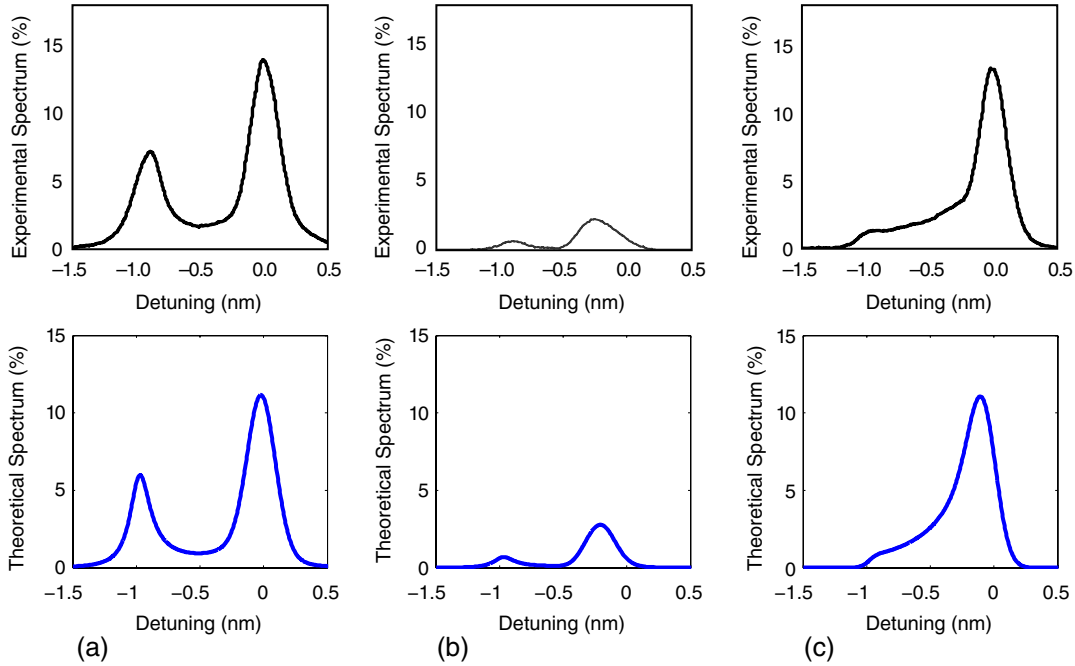

Fig. 3. (Color online) Comparison of measured drop-port spectra from [3] with theoretical drop-port spectra predicted by Eq. (14) for three different experimental scenarios: (a) absorbed pump energy of 0.7 pJ, (b) probe pulses detuned from resonance by 0.25 nm, (c) pump pulses broadened to 26 ps duration. In (c) a pump-probe delay of 20 ps was chosen. No other fitting parameters were used in the simulations; all of the necessary information was reported in [3] and is recorded in Table 1. The experimental spectra are adapted from [3] with permission from Macmillan Publishers Ltd., copyright 2007.

good agreement, there are some quantitative differences between the experimentally measured spectra and the predictions of our model. The overall relative drop-port efficiency predicted by the model is lower by about 25% than what was observed in the experiment, and the predicted extent of the wavelength shift is also slightly different from the measured results. There are many possible reasons for these quantitative differences. For example, to our knowledge no definitive experiment has been done to test the accuracy of the semiempirical model for the free-carrier index change in Eq. (22). In addition, the calculated spectra depend on several experimental parameters, all of which were measured with some degree of uncertainty. In our opinion, the degree of quantitative and qualitative agreement between the calculated and measured spectra is remarkable given the complete absence of fitting parameters and the number of possible sources of error.

Figure 3 tests the predictions of our theory when parameters other than the pump-pulse energy are varied. For each of these scenarios, a value of 0.7 pJ for the absorbed pump-pulse energy was taken from the plot in Fig. 3 of [3]. Part (a) shows the output spectrum under the same experimental conditions that were used for Fig. 2 except for the value of the pump-pulse energy. Part (b) shows the output spectrum when the input probe pulse is detuned from resonance by 0.25 nm. In this case, the converted signal is weak because relatively little of the probe pulse couples into the resonator at the detuned wavelength. Part (c) shows the output spectrum when the wavelength of the probe pulse is unchanged, but the pump pulse has been broadened to a duration of 26 ps so that the index change occurs on a time scale longer than the 15.5 ps photon lifetime of the resonator. As mentioned before, since the delay between the peak of the pump pulse and the peak of the incident probe pulse was not provided in [3] for this last experiment, a value of 20 ps was chosen. AWC efficiency is considerably reduced in this case because the probe pulse leaks out of the resonator before it has been fully converted to the new wavelength. As was the case in Fig. 2, other than a discrepancy in AWC efficiency, the predicted spectra are in remarkably good agreement with the experimental data.

Table 1. Parameter Values [a] Used for Figs. 2 and 3

Quality factor (Q)	18, 614
Ring diameter	6 μm
Cavity volume (V_{cav})	2.12 μm^3
Probe wavelength (λ)	1.564 μm
Pump wavelength (λ_p)	0.415 μm
Probe pulse width	18 ps
Pump-pulse width	0.1 ps
Absorption efficiency (ξ)	0.07
Pump-probe delay	13.2 ps

[a]Taken or deduced from [3].

4. DYNAMIC MODE COUPLING

Dynamic mode coupling results in the transfer of energy stored in one resonator mode to neighboring modes through dynamic refractive index changes. Physically, even if the input field is tuned to excite only a single resonance, dynamic index changes can be used to create an output spectrum that spans multiple resonances. Since the longitudinal modes of a resonator are uniformly spaced in frequency, the output appears in the form of a frequency comb.

A. Interpretation of the Dynamical Equations

The transfer of optical energy from a single resonator mode to neighboring modes occurs only under certain conditions.

Mathematically, this phenomenon is described through the off-diagonal matrix elements (Γ_{km} for $m \neq k$) in Eq. (11). These off-diagonal elements introduce coupling among various resonator modes oscillating at different frequencies and produce a transfer of energy from a resonantly excited mode into its nearest spectral neighbors.

Dynamic mode coupling will happen efficiently only if index changes occur on a time scale comparable to or shorter than the reciprocal of the mode-spacing $\Delta_{km} = \omega_k - \omega_m$. This is most clearly understood from the approximation to the dynamic mode-amplitude equation, Eqs. (13). In order for mode m to efficiently transfer energy to mode k the term $i\Gamma_{km}\omega_m a_m$, which appears in the equation for the kth mode's amplitude, must have spectral components which are frequency-matched to the kth mode's resonance frequency ω_k. Since a_m oscillates at ω_m this leads to the requirement that Γ_{km}, and hence the refractive index, change on a time scale shorter than $1/\Delta_{km}$. In the case of the nearest neighbors, we can equivalently say that energy transfer will occur only if the index changes on a time scale comparable to or shorter than the round-trip time τ_r of the resonator.

A second condition that is necessary for dynamic mode coupling to occur is that the dynamic refractive index changes be spatially nonuniform. This is inferred from the definition of Γ_{km} in Eq. (12) and the spatial symmetry properties of the mode profiles. Consider as an example the ring resonator depicted in Fig. 4 for which the refractive index is changed uniformly over a fraction of the ring perimeter denoted by f (indicated by purple when viewed in color). In a cylindrical coordinate system whose origin is at the center of the ring and whose z axis is normal to the substrate, the electric field of the kth mode has the form

$$\mathbf{e}_k(r,\theta,z) = E_k\mathbf{u}(r,\theta,z)e^{ik\theta}. \tag{25}$$

Here $\mathbf{u}(r,\theta,z)$ is the transverse profile of the waveguide mode. Note that it is only the orientation of $\mathbf{u}$ which depends on θ, and the magnitude $|\mathbf{u}|$ depends only on r and z. Thus we can choose $\mathbf{u}$ to be normalized such that $\iint r|\mathbf{u}|^2 dr dz = 1$. If we assume that the mode profile is independent of frequency over the spectral range of interest, the coupling coefficient given in Eq. (12) is found to be

$$\Gamma_{km} = (f/n_0)\Delta n(t)\mathrm{sinc}[(m-k)\pi f]e^{i(m-k)\pi f}, \tag{26}$$

where $\mathrm{sinc}(x) = \sin x/x$.

We see from Eq. (26) that all off-diagonal coupling terms vanish for a spatially uniform index change ($f = 1$) over the entire resonator, and no energy transfer can occur in that situation. Equation (26) also indicates that the fraction of the resonator length over which index changes occur determines the number of neighboring modes to which a given mode will efficiently couple. If the index is changed over 1/3 of the resonator, for example, then a given mode will couple effectively to its four nearest neighbors, two on the blue side and two on the red side. For modes that are further away than this, Γ_{km} is negligible in comparison. The phenomenon of mode coupling by dynamic refractive index changes was first studied using numerical FDTD simulations in [1] and verified experimentally later by Dong *et al.* [15]. The requirement of a sufficiently fast and nonuniform index change was noted in each of these studies.

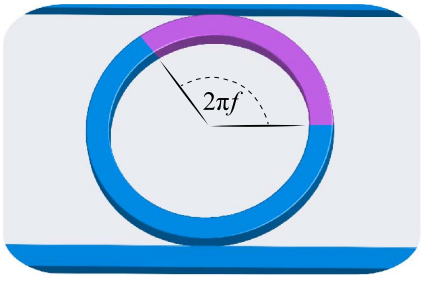

Fig. 4. (Color online) Ring-resonator configuration for dynamic mode coupling. The arc along the ring (purple region when viewed in color) indicates the portion of the resonator over which the refractive index is changed.

B. Comparison with Experimental Results

To test the validity or our model in the case of dynamic mode coupling, we compare its predictions with the experimental results presented in [15]. The experiment was very similar to the one in [3] that we studied in Section 3, except for two fundamental differences. First, a much larger ring resonator was used (with a diameter of 100 μm) so that the spot size of the focused pump pulses would be smaller than the size of the ring, resulting in a nonuniform distribution of generated free carriers, and therefore in a spatially nonuniform index change. Second, a CW probe beam was used instead of a pulsed probe beam.

To model this experiment, we solved Eq. (11) together with the carrier rate equation (23) and the semiempirical model for the free-carrier induced index change described in Eq. (22). The coupling coefficients Γ_{km} were calculated using Eq. (26). The only two parameters required for modeling the experiment and not explicitly reported in [15] are the pump-cavity overlap fraction f and the pump absorption efficiency ξ. If we assume that the spot size of the focused pump pulses (W_{pump}) is 10 μm, as was previously reported by the same group in [3], then we can calculate the fraction f in terms of the ring diameter D as $f \approx W_{\mathrm{pump}}/\pi D$, leading to $f = 1/30$ for the 100 μm diameter ring used in the experiment. The fraction ξ can be induced by fitting the experimental data in Fig. 2(e) in [15] showing a measurement of the adiabatic wavelength shift of each of the cavity modes as a function of pump-pulse energy. The expected adiabatic wavelength shift from our model is $\Delta\lambda = \Gamma\lambda_0$, where $\Gamma = f\Delta n/n_0$ from Eq. (26). In order to fit their experimental plot to our model we find that $\xi = 0.07$, which is exactly the same as the value of ξ reported previously in [3]. This suggests that we have accurately induced the correct values of both f and ξ for modeling their experimental results. All other parameters used in the numerical simulation are taken from [15] and summarized in Table 2.

Figure 5 compares (a) the experimental spectrum at the drop port of the resonator [15] with (b) the spectrum predicted by our model. The spectral peak at 1567.5 nm is that of the CW probe beam which is initially on resonance. After the arrival of the 200 fs pump pulses, a part of the energy of this resonant probe beam is adiabatically shifted to a new resonance frequency about 1 nm to the blue side of the spectrum (AWC). Another part of the energy is coupled into several neighboring modes, which are also spectrally blue-shifted from their initial resonance frequencies. In the experimental spectrum, these initial resonances could be observed because the CW probe

Table 2. Parameter Values [a] Used for Fig. 5

Quality factor (Q)	12, 000
Ring diameter	100 μm
Cavity volume (V_{cav})	35.3 μm^3
Free-spectral range	1.9 nm
Probe wavelength (λ)	1.5675 μm
Pump wavelength (λ_p)	0.412 μm
Pump-pulse width	0.200 ps
Pump-pulse energy (E_p)	300 pJ
Absorption efficiency (ξ)	0.07
Pump-cavity overlap fraction (f)	1/30

[a]Taken from [15]. The values of f and ξ were induced from statements made in [3].

beam had broadband noise imposed on it (most likely by an amplifier). In the theoretical spectrum the initial resonances are not observable because no noise is taken into account for the input beam. We have added a noise floor to the output beam at −65 dB below the central peak in order to take into account as much of the experimental scenario as possible.

As the blue-shifted spectral peaks associated with the cavity modes in Fig. 5(a) are much larger than the peaks at the initial resonance frequencies, one can conclude that their origin lies in the mode-coupling phenomenon (and is not related to AWC). The relative excitation amplitudes of these neighboring modes in the theoretical spectrum are in good agreement with what was observed in the experiment. One source of error in numerical simulations results from a finite number of modes used in the calculation. We used nine modes in our calculation so that the spectrum is reasonably accurate over the span of the seven modes presented in Fig. 5. In addition to this, a simulation time window of only 1.6 ns was used, which is considerably smaller than the 13.2 ns repetition period of the pump pulses in the experiment. In spite of these limitations, the overall agreement seen in Fig. 5 indicates that our theoretical model can predict the experimental behavior quite well.

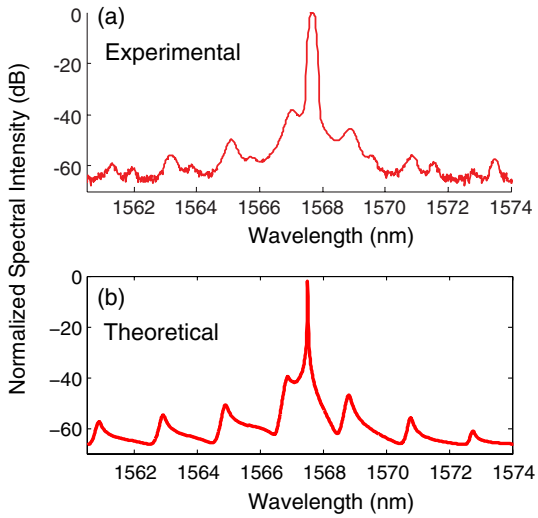

Fig. 5. (Color online) Mode coupling in a silicon ring resonator undergoing spatially nonuniform refractive index changes. The (a) drop-port spectrum measured in [15] is compared with the (b) predicted spectrum under the same experimental conditions. Simulation parameters are recorded in Table 2. No fitting parameters were used in the calculation. Figure 5(a) is adapted from [15] with permission from the American Physical Society, copyright 2008.

5. CONCLUSIONS

In this paper we have developed a theoretical model for the dynamics of an optical field in a dielectric resonator which is undergoing refractive index changes. We used an operator formulation of Maxwell's equations that enables us to write them in the form of the well-known Schrödinger equation. The resonant modes of a cavity correspond to the eigenstates of an operator that appears in this equation, while dynamic changes in the refractive index were treated as perturbations to these resonant modes. With this approach, the use of the standard time-dependent perturbation theory led to a set of coupled differential equations for various mode amplitudes. The dynamic coupling matrix $\Gamma_{km}(t)$ appearing in these equations accounts for all novel physical processes that can be expected to occur. In particular, we found that the AWC process is controlled by the diagonal elements of this matrix, and that the off-diagonal terms are responsible for the transfer of energy from a specific excited mode to its neighboring modes. Our model shows clearly that the latter process can occur only when the index changes are spatially nonuniform. We discussed the cases of spatially uniform and nonuniform index changes separately and compared the predictions of our model with experimental data available in the literature. The overall good agreement suggests that our model should be useful for studying the dynamics of optical fields in resonators undergoing perturbation. Since no assumptions are made about the type of dielectric cavity used or the temporal structure of the input field, this model should be applicable to a wide range of experimental scenarios.

APPENDIX A: INCORPORATION OF THE FINITE PHOTON LIFETIME AND INPUT COUPLING

In this appendix we discuss the origin of two terms in the mode-amplitude Eq. (9) that take into account cavity losses (leading to a finite photon lifetime) and coupling of the resonator to an external input field. These terms are often included on intuitive heuristic grounds [22]. We attempt to re-enforce this intuition with a mathematical framework. We will derive the dynamical equation which a given mode-amplitude a_k is expected to obey in the absence of the perturbing dipole-moment density $\mathbf{P}^{(p)}$ and in the presence of loss and coupling to an external field. For this purpose we define a mode-power amplitude A_k through the relation

$$a_k(t) = \sqrt{\tau_r} A_k(t) e^{-i\omega_0 t}. \tag{A1}$$

With this definition, $|A_k|^2$ is the optical power carried by the kth mode at some location in the cavity. Here, ω_0 is the carrier frequency of the input field; it may be detuned from a cavity resonance by $\Delta\omega = \omega_0 - \omega_k$. It is also useful to define a slowly varying amplitude A'_{in} for the input field using

$$A_{in}(t) = A'_{in}(t) e^{-i\omega_0 t}. \tag{A2}$$

By considering how the mode-amplitude A_k changes over one round trip inside the resonator, we obtain

$$A_k(t) = \sqrt{\eta_k} A_k(t - \tau_r) e^{i\Delta\omega\tau_r} + \sqrt{T_k} A'_{in}(t), \tag{A3}$$

where η_k is the fraction of power retained by the kth mode after one round trip and is close to 1 for high-Q cavities. $\Delta\omega\tau_r$ is the phase acquired by this mode as a result

of detuning from the resonance frequency. By assuming that the amplitude A_k does not vary appreciably over a single round trip so that

$$\frac{dA_k}{dt} \approx \frac{A_k(t) - A_k(t-\tau_r)}{\tau_r},$$

we can approximate Eq. (A3) by the following differential equation:

$$\frac{dA_k}{dt} = -\frac{1}{\tau_r \sqrt{\eta_k}}\left(e^{-i\Delta\omega\tau_r} - \sqrt{\eta_k}\right)A_k + \frac{\sqrt{T_k}}{\tau_r \sqrt{\eta_k}} A'_{in} e^{-i\Delta\omega\tau_r}. \quad \text{(A4)}$$

Finally, we make use of the identities in Eqs. (A1) and (A2) with the approximations $|\Delta\omega\tau_r| \ll 1$ and $\sqrt{\eta_k} \approx 1$ and obtain the following dynamical equation for the energy amplitude a_k:

$$\frac{da_k}{dt} = -i\omega_k a_k - \frac{1}{2\tau_{ph}^k} a_k + \kappa_k A_{in}, \quad \text{(A5)}$$

where $1/\tau_{ph}^k = (1-\eta_k)/\tau_r$. Equation (A5) is identical to Eq. (9) in the absence of the perturbation term.

ACKNOWLEDGMENTS

This work was supported in part by the National Science Foundation (NSF) through the awards ECCS-0801772 and ECCS-1041982. We also acknowledge fruitful discussions with Yuzhe Xiao on this topic.

REFERENCES

1. M. Notomi and S. Mitsugi, "Wavelength conversion via dynamic refractive index tuning of a cavity," Phys. Rev. A **73**, 051803 (2006).
2. M. F. Yanik and S. Fan, "Dynamic photonic structures: stopping, storage, and time reversal of light," Stud. Appl. Math. **115**, 233–253 (2005).
3. S. F. Preble, Q. Xu, and M. Lipson, "Changing the colour of light in a silicon resonator," Nat. Photon. **1**, 293–296 (2007).
4. S. F. Preble and M. Lipson, "Conversion of a signal wavelength in a dynamically tuned resonator," in *Integrated Photonics Research and Applications/Nanophotonics*, Technical Digest (CD) (Optical Society of America, 2006), paper IMC5.
5. Z. Gaburro, M. Ghulinyan, F. Riboli, L. Pavesi, A. Recati, and I. Carusotto, "Photon energy lifter," Opt. Express **14**, 7270–7278 (2006).
6. T. Kampfrath, D. M. Beggs, T. P. White, A. Melloni, T. F. Krauss, and L. Kuipers, "Ultrafast adiabatic manipulation of slow light in a photonic crystal," Phys. Rev. A **81**, 043837 (2010).
7. Y. Xiao, D. N. Maywar, and G. P. Agrawal, "Optical pulse propagation in dynamic Fabry-Perot resonators," J. Opt. Soc. Am. B **28**, 1685–1692 (2011).
8. M. W. McCutcheon, A. G. Pattantyus-Abraham, G. W. Rieger, and J. F. Young, "Emission spectrum of electromagnetic energy stored in a dynamically perturbed optical microcavity," Opt. Express **15**, 11472–11480 (2007).
9. Q. Lin, T. J. Johnson, C. P. Michael, and O. Painter, "Adiabatic self-tuning in a silicon microdisk optical resonator," Opt. Express **16**, 14801–14811 (2008).
10. T. Tanabe, M. Notomi, H. Taniyama, and E. Kuramochi, "Dynamic release of short pulse from ultrahigh-Q nanocavities via adiabatic wavelength conversion," in *Conference on Lasers and Electro-Optics*, Technical Digest (CD) (Optical Society of America, 2008), paper QPDB1.
11. T. Tanabe, M. Notomi, H. Taniyama, and E. Kuramochi, "Dynamic release of trapped light from an ultrahigh-Q nanocavity via adiabatic frequency tuning," Phys. Rev. Lett. **102**, 043907 (2009).
12. A. W. Elshaari and S. F. Preble, "Active optical isolator using adiabatic wavelength conversion in microcavities," in *Frontiers in Optics*, Technical Digest (CD) (Optical Society of America, 2009), paper FThU4.
13. E. E. Hach, III, A. W. Elshaari, and S. F. Preble, "Fully quantum-mechanical dynamic analysis of single-photon transport in a single-mode waveguide coupled to a traveling-wave resonator," Phys. Rev. A **82**, 063839 (2010).
14. Y. Xiao, G. P. Agrawal, and D. N. Maywar, "Spectral and temporal changes of optical pulses propagating through time-varying linear media," Opt. Lett. **36**, 505–507 (2011).
15. P. Dong, S. F. Preble, J. T. Robinson, S. Manipatruni, and M. Lipson, "Inducing photonic transitions between discrete modes in a silicon optical microcavity," Phys. Rev. Lett. **100**, 033904 (2008).
16. J. W. Winn, S. Fan, J. D. Joannopoulos, and E. P. Ippen, "Interband transitions in photonic crystals," Phys. Rev. B **59**, 1551–1554 (1999).
17. N. Malkova, S. Kim, and V. Gopalan, "Jahn-Teller effect in two-dimensional photonic crystals," Phys. Rev. B **68**, 045105 (2003).
18. Y. Xu, Y. Li, R. K. Lee, and A. Yariv, "Scattering-theory analysis of waveguide-resonator coupling," Phys. Rev. E **62**, 7389–7404 (2000).
19. Q. Lin, T. J. Johnson, R. Perahia, C. P. Michael, and O. J. Painter, "A proposal for highly tunable optical parametric oscillation in silicon micro-resonators," Opt. Express **16**, 10596–10610 (2008).
20. T. J. Johnson, "Silicon microdisk resonators for nonlinear optics and dynamics," Ph.D. dissertation (California Institute of Technology, 2009).
21. R. A. Soref and B. R. Bennett, "Electrooptical effects in silicon," IEEE J. Quantum Electron. **23**, 123–129 (1987).
22. H. A. Haus, *Waves and Fields in Optoelectronics* (Prentice-Hall, 1984).